

Simulation of Electron Cooling Process in a Storage Ring

Rao Yinong, Xia Jiawen, Yuan Youjin, and Wei Baowen

(Institute of Modern Physics, The Chinese Academy of Sciences, Lanzhou, China)

A simulation of the electron cooling process for the heavy ion beam in the proposed HIRFL cooler-storage ring (HIRFL-CSR) is performed by taking into account the betatron and synchrotron oscillations of single particles. The continuous evolution of ion beam emittances and relative momentum spread are given. Some factors that influence the cooling time, like the space charge effect of the electron beam, the dispersion in the cooling section, and the electron beam transverse temperature are presented.

Key words: electron cooling, cooling force, cooling time, betatron oscillation, synchrotron oscillation.

1. INTRODUCTION

The electron cooling time and its dependence on some other parameters must be known in the design of the cooling scheme and studies on beam properties in a cooler ring, because the cooling time characterizes the speed of cooling. Generally, calculation of the cooling time is based upon the cooling force. However, the complicated dependence of cooling force on parameters brings difficulties to an analytical calculation of the cooling process. Consequently, the approximate formula [1-3] below is frequently used to estimate the time of cooling for betatron amplitude

$$t_c = - \left(\frac{1}{v_i} \frac{dv_i}{dt} \right)^{-1} = C \cdot \frac{A_i}{Q_i^2} \cdot \frac{\beta_i^4 \gamma_i^5}{\eta_{ec} \cdot j_c} \cdot (\theta_i^2 + \theta_c^2)^{\frac{3}{2}}, \quad (1)$$

Received February 15, 1996.

© 1997 by Allerton Press, Inc. Authorization to photocopy individual items for internal or personal use, or the internal or personal use of specific clients, is granted by Allerton Press, Inc. for libraries and other users registered with the Copyright Clearance Center (CCC) Transactional Reporting Service, provided that the base fee of \$50.00 per copy is paid directly to CCC, 222 Rosewood Drive, Danvers, MA 01923.

in which β_i and γ_i are relativistic factors of the ion with charge state Q_i and mass number A_i , θ_e , and θ_i are divergences of the electron and ion beam in the cooling section, respectively, j_e is the electron current density in A/cm² and η_{ec} is the ratio of cooling section length to the ring circumference. The constant C in Eq. (1) assumes much different values in different references. Moreover, the above expression, in some cases, gives only an instantaneous value without taking into account the peculiarities of the motion such as the periodical oscillation of particles in focusing and RF system of a storage ring. When one tries to consider these effects, a simple analytical calculation seems to be impossible.

This paper is devoted to the simulation of the electron cooling process for a bunched ion beam Ar^{18+} of 25 MeV/u in the proposed HIRFL-CSR with the use of the analytical cooling force formulas, and with consideration of the betatron and synchrotron oscillations of single particles, the influence of electron beam space charge [4], and dispersion in the cooling section. The continuous evolution of beam emittances and momentum spread obtained from the simulation are shown as functions of time. Afterwards, some factors that influence the cooling speed are described.

2. DESCRIPTION OF THE SIMULATION PROCESS

2.1. Betatron and synchrotron oscillation

In the simulation procedure, the ring is divided into two parts: the first part is from the exit of the cooling section (labeled with subscript 0) to its entrance (labeled with subscript 1), and the second goes through the cooling section. After one turn in the ring, the phase of the inspected ion with respect to RF and its relative momentum spread are described by the phase motion equations [5]

$$\left\{ \begin{array}{l} \frac{d\phi}{dt} = h\omega_s \cdot \eta_p \cdot \frac{\Delta p}{p_s}, \\ \frac{d}{dt} \left(\frac{\Delta p}{p_s} \right) = \frac{\omega_s}{2\pi} \cdot \frac{Q_i e U_a}{A_i M_N c^2 \beta_i^2 \gamma_i} \cdot (\cos\phi - \cos\phi_s), \end{array} \right. \quad (2)$$

where h is the RF harmonic number, ω_s and ϕ_s are the revolution angular frequency and phase of the synchronous ion, respectively, $\eta_p = \frac{1}{\gamma_i^2} - \frac{1}{\gamma_{tr}^2}$, γ_{tr} is the transition energy factor of the ring, U_a is the amplitude of RF voltage, $M_N c^2 = 931.501$ MeV/u is rest energy per nucleon, c is the speed of light, and e is the electron charge.

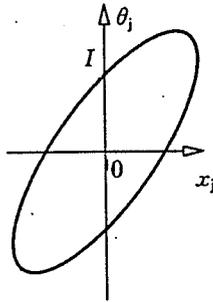


Fig. 1
Transverse betatron ellipse of ion beam.

From Eqs. (2) and (3), one gets the phase and momentum spread of the ion at the entrance of the cooling section

$$\phi_1 = \phi_0 + 2\pi(1 - \eta_{ec}) \cdot h \cdot \eta_p \cdot \left(\frac{\Delta p}{p_s} \right)_0, \tag{4}$$

$$\left(\frac{\Delta p}{p_s} \right)_1 = \left(\frac{\Delta p}{p_s} \right)_0 + \frac{Q_i e U_a}{A_i M_N c^2 \beta_i^2 \gamma_i} \cdot (1 - \eta_{ec}) \cdot (\cos \phi_1 - \cos \phi_0), \tag{5}$$

While the transverse betatron positions and divergences after the first part are given by the following matrix expression [6]

$$\begin{pmatrix} x_j \\ \theta_j \end{pmatrix}_1 = \begin{bmatrix} \cos(\mu_j) + \alpha_j \sin(\mu_j) & \beta_j \sin(\mu_j) \\ -\gamma_j \sin(\mu_j) & \cos(\mu_j) - \alpha_j \sin(\mu_j) \end{bmatrix} \cdot \begin{pmatrix} x_j \\ \theta_j \end{pmatrix}_0, \tag{6}$$

in which $j = h, v$ designates horizontal and vertical, respectively, $\mu_j = 2\pi\nu_j(1 - \eta_{ec})$ is the betatron phase shift of the inspected ion after the first part, $\nu_j = Q_j + \xi_j \cdot \frac{\Delta p}{p_s}$, ν_j and Q_j are betatron wave numbers of the inspected ion and the synchronous ion, respectively, ξ_j is the chromaticity of machine, $\alpha_j, \beta_j,$ and γ_j are Twiss parameters at the entrance or exit of the cooling section (symmetric points).

One assumes that the ion is initially located at point I of the transverse phase ellipse shown in Fig. 1, the betatron position and divergence correspond to

$$\begin{pmatrix} x_j \\ \theta_j \end{pmatrix}_0 = \begin{pmatrix} 0 \\ \sqrt{\frac{\epsilon_{j0}}{\pi\beta_j}} \end{pmatrix}, \tag{7}$$

where $\pi\epsilon_{j0}$ is the initial emittance.

On each passage through the cooling section, the ion experiences a cooling force which decreases the velocity components but does not change the position coordinates evidently. In the lab frame, the cooling differential equations are expressed as

$$\frac{dp}{ds} = F \cdot \frac{dt}{ds} = \frac{F}{\beta_i c}, \quad 0 \leq s \leq L_{\text{cooler}},$$

$$\frac{dp_j}{p_s} \cdot \frac{1}{ds} = \frac{F_j}{p_s \cdot \beta_i c}$$

$$\frac{d\theta_j}{ds} = \frac{F_j}{A_i M_N c^2 \beta_i^2 \gamma_i}, \tag{8}$$

$$\frac{d}{ds} \left(\frac{\Delta p}{p_s} \right) = \frac{F_1}{A_i M_N c^2 \beta_i^2 \gamma_i}. \tag{9}$$

in which $0 \leq s \leq L_{\text{cooler}}$, L_{cooler} is the length of cooling section. F_j and F_l denote transverse and longitudinal cooling forces, respectively.

By means of numerical integration for Eqs. (8) and (9), one can obtain θ_j and $\frac{\Delta p}{p_s}$ values at the exit of the cooling section. In the practical evaluation, the different method is used to solve the above equations, i.e.,

$$\delta\theta_j = \frac{F_j}{A_i M_N c^2 \beta_i^2 \gamma_i} \cdot \delta s, \quad \delta \left(\frac{\Delta p}{p_s} \right) = \frac{F_l}{A_i M_N c^2 \beta_i^2 \gamma_i} \cdot \delta s.$$

where δs is chosen such that $|\delta\theta_j| \leq 0.05|\theta_j|$ and $\left| \delta \left(\frac{\Delta p}{p_s} \right) \right| \leq 0.05 \left| \frac{\Delta p}{p_s} \right|$, [7]. Following this criteria, the cooling section is divided successively into two equal segments. After each subsegment, the divergence and momentum spread are changed into $\theta_j + \delta\theta_j$ and $\frac{\Delta p}{p_s} + \delta \left(\frac{\Delta p}{p_s} \right)$, which are taken as the starting values for the next segment, up to passing through the entire cooling section.

After traversal of the cooling section, the betatron phase and position of the ion are approximately unchanged, i.e.,

$$\phi_i \simeq \phi_0, \quad (x_j)_i \simeq (x_j)_0.$$

2.2. Cooling force

As mentioned above, the behavior of the ion after transmission through the cooling section depends on the cooling force. In a frame moving with the electron average velocity (labeled with superscript 'm'), the cooling forces are expressed as [7]

$$F_j^m = -2\pi n_e \cdot Q_i^2 r_e^2 \cdot m_e c^4 \cdot v_j \cdot \begin{cases} \frac{1}{v^3} \left(2L_{\text{FH}} + \frac{v_t^2 - 2v_l^2}{v^2} \cdot L_{\text{MH}} \right), & v > \Delta_t \\ \frac{2}{\Delta_t^3} (L_{\text{FL}} + N_L L_{\text{AL}}) + \frac{v_t^2 - 2v_l^2}{v^2} \cdot \frac{L_{\text{ML}}}{v^3}, & \Delta_t < v < \Delta_l \\ \frac{2}{\Delta_t^3} (L_{\text{FS}} + N_S L_{\text{AS}}) + \frac{L_{\text{MS}}}{\Delta_t^3}, & v < \Delta_t \end{cases}$$

$$F_l^m = -2\pi n_e \cdot Q_i^2 r_e^2 \cdot m_e c^4 \cdot v_l \cdot \begin{cases} \frac{1}{v^3} \left(2L_{\text{FH}} + \frac{3v_t^2}{v^2} \cdot L_{\text{MH}} + 2 \right), & v > \Delta_t \\ \frac{2}{\Delta_t^3 v_l} (L_{\text{FL}} + N_L L_{\text{AL}}) + \left(\frac{3v_t^2}{v^2} \cdot L_{\text{ML}} + 2 \right) \cdot \frac{1}{v^3}, & \Delta_t < v < \Delta_l \\ \frac{2}{\Delta_t^3 \Delta_l} (L_{\text{FS}} + N_S L_{\text{AS}}) + \frac{L_{\text{MS}}}{\Delta_l^3}, & v < \Delta_t \end{cases}$$

in which n_e is the electron density, r_e and m_e are classical radius and rest mass of the electron, respectively, v_t and v_l are transverse and longitudinal velocities of ion, while Δ_t and Δ_l are transverse and longitudinal rms velocities of electron beam, respectively, and 'L' denotes the Coulomb logarithm [7]. All of these quantities are measured in the moving frame.

Considering the flattened velocity distribution [8] due to the electrostatic acceleration, and the longitudinal temperature growth due to the longitudinal-longitudinal relaxation [9], the electron beam rms velocities can be deduced from its relevant temperatures by

$$kT_i = m_e \Delta_i^2, \quad kT_l = m_e \Delta_l^2 = \frac{(kT_i)^2}{m_e c^2 \beta_i^2 \gamma_i^2} + \frac{e^2 n_e^{1/3}}{4\pi \epsilon_0},$$

where k is the Boltzmann constant and ϵ_0 is the permittivity of free space.

For convenience of calculation, one changes velocities in the moving frame to divergences in the lab frame by

$$\Delta_i = \beta_i \gamma_i c \cdot \theta_{ei}, \quad \Delta_l = \beta_l \gamma_l c \cdot \theta_{el},$$

$$v_h = \beta_i \gamma_i c \cdot \theta_h, \quad v_v = \beta_i \gamma_i c \cdot \theta_v, \quad u = \beta_i \gamma_i c \cdot \theta_1 = \beta_i \gamma_i c \cdot \left(\frac{1}{\gamma_i} \frac{\Delta p}{p_s} \right),$$

Consequently, one gets

$$v = \sqrt{v_h^2 + v_v^2 + v_l^2} = \beta_i \gamma_i c \cdot \sqrt{\theta_h^2 + \theta_v^2 + \theta_l^2} = \beta_i \gamma_i c \cdot \theta,$$

$$\frac{v_i^2 - 2v_l^2}{v^2} = 1 - 3 \left(\frac{\theta_l}{\theta} \right)^2, \quad \frac{3v_l^2}{v^2} = 3 - 3 \left(\frac{\theta_l}{\theta} \right)^2,$$

Moreover, by transforming the cooling force components from the moving frame to the lab frame (labeled with superscript 'l') and by relating the electron density n_e in the moving frame to the electron beam radius r_b and electron current I_e in the lab frame

$$F_j^l = \frac{1}{\gamma_i} \cdot F_j^m, \quad F_l^l = F_l^m,$$

$$n_e = \frac{I_e}{\pi r_b^2 \cdot e \beta_i \gamma_i c},$$

one finally obtains the expressions of cooling force in the lab frame

$$F_j^l = -2\pi \cdot \frac{I_e}{\pi r_b^2 \cdot e \beta_i \gamma_i c} \cdot Q_i^2 r_e^2 \cdot m_e c^2 \cdot \frac{\bar{\theta}_j}{\beta_i^2 \gamma_i^3}$$

$$\cdot \begin{cases} \frac{1}{\theta^3} (2L_{FH} + K_t \cdot L_{MH}), & \theta > \theta_{ei} \\ \frac{2}{\Delta_{ei}^3} (L_{FL} + N_L L_{AL}) + K_t \cdot \frac{L_{ML}}{\theta^3}, & \theta_{el} < \theta < \theta_{ei}; \\ \frac{2}{\theta_{ei}^3} (L_{FS} + N_S L_{AS}) + \frac{L_{MS}}{\theta_{ei}^3}, & \theta < \theta_{ei} \end{cases}$$

$$F_1^1 = -2\pi \cdot \frac{I_c}{\pi r_b^2 \cdot e\beta_i\gamma_i c} \cdot Q_i^2 r_c^2 \cdot m_e c^2 \cdot \frac{\theta_1}{\beta_i^2 \gamma_i^2}$$

$$\cdot \begin{cases} \frac{1}{\theta^3} (2L_{FH} + K_1 \cdot L_{MH} + 2), & \theta > \theta_{ct} \\ \frac{2}{\theta_{ct}^2 \theta_1} (L_{FL} + N_L L_{AL}) + (K_1 \cdot L_{ML} + 2) \cdot \frac{1}{\theta^3}, & \theta_{cl} < \theta < \theta_{ct}, \\ \frac{2}{\theta_{ct}^2 \theta_{cl}} (L_{FS} + N_S L_{AS}) + \frac{L_{MS}}{\theta_{cl}^3}, & \theta < \theta_{cl} \end{cases}$$

in which

$$K_1 = 1 - 3 \left(\frac{\theta_1}{\theta} \right)^2, \quad K_1 = 3 - 3 \left(\frac{\theta_1}{\theta} \right)^2,$$

and the Coulomb logarithms are given as follows

$$L_{FH} = \ln \left(\frac{\beta_i^3 \gamma_i^3 c \theta^3}{Q_i \omega_c r_c} \right), \quad L_{MH} = \max \left[\ln \left(\frac{\omega_c}{\omega_{pe}} \cdot \frac{\theta}{\theta_{ct}} \right), \ln \left(\frac{\omega_c}{\beta_i \gamma_i c \theta_{ct}} \cdot \left(\frac{3Q_i}{n_e} \right)^{1/3} \right) \right],$$

$$L_{FL} = \ln \left(\frac{\beta_i^3 \gamma_i^3 \theta_{ct}^2 \theta}{Q_i \omega_c r_c} \right), \quad L_{AL} = \ln \left(\frac{\theta_{ct}}{\theta} \right),$$

$$L_{ML} = L_{MH}, \quad L_{FS} = \ln \left(\frac{\beta_i^3 \gamma_i^3 c \theta_{ct}^2 \theta_{cl}}{Q_i \omega_c r_c} \right),$$

$$L_{AS} = \ln \left(\frac{\theta_{ct}}{\theta_{cl}} \right), \quad L_{MS} = \max \left[\ln \left(\frac{\omega_c}{\omega_{pe}} \cdot \frac{\theta_{cl}}{\theta_{ct}} \right), \ln \left(\frac{\omega_c}{\beta_i \gamma_i c \theta_{ct}} \cdot \left(\frac{3Q_i}{n_e} \right)^{1/3} \right) \right],$$

$$N_L = \left[\frac{\theta_{ct}}{\pi \theta} \right], \quad N_S = \left[\frac{\theta_{ct}}{\pi \theta_{cl}} \right].$$

where $\omega_c = \frac{eB}{m_e}$ is the angular frequency of electron rotating around the longitudinal solenoid field B ,

and $\omega_{pe} = \sqrt{n_e \cdot 4\pi r_c} \cdot c$ is the frequency of electron plasma.

Because of the electron beam space charge depression, electrons at different radii inside the beam have different longitudinal velocities. Accordingly, the longitudinal velocity component of an ion at certain radius should be defined with respect to that of an electron at the same radius.

Following the electrostatic Gaussian theorem, one finds the radial electric field at radius r

$$E = - \frac{I_c}{2\pi \epsilon_0 r_b^2 \cdot \beta_i c} \cdot r, \quad 0 \leq r \leq r_b,$$

which results in a potential difference

$$\Delta U = - \int_0^r E \cdot dr = \frac{I_c}{2\pi \epsilon_0 \beta_i c} \cdot \frac{r^2}{r_b^2},$$

Therefore, the relative energy deviation of an electron at radius r from that on the axis is given by

$$\frac{\Delta W_e}{W_s} = \frac{e \cdot \Delta U}{m_e c^2 (\gamma_i - 1)} = \frac{I_e}{2\pi\epsilon_0\beta_i c} \cdot \frac{e}{m_e c^2 (\gamma_i - 1)} \cdot \frac{r^2}{r_b^2},$$

so the relative momentum deviation is

$$\frac{\Delta p_e}{p_s} = \frac{\gamma_i}{\gamma_i + 1} \frac{\Delta W_e}{W_s} = \frac{I_e}{2\pi\epsilon_0\beta_i^3 c} \cdot \frac{e}{m_e c^2 \gamma_i} \cdot \frac{r^2}{r_b^2}. \quad (10)$$

Signifying f_n the neutralization factor of space charge, one gets the divergence deviation θ_1^n

$$\begin{aligned} \theta_1^n &= \theta_1 - \frac{1}{\gamma_i} \frac{\Delta p_e}{p_s} \\ &= \theta_1 - \frac{I_e}{2\pi\epsilon_0\beta_i^3 c} \cdot \frac{e}{m_e c^2 \gamma_i^2} \cdot \frac{r^2}{r_b^2} \cdot (1 - f_n), \end{aligned}$$

in which the radius r is related to the horizontal dispersion D_h in the cooling section by

$$r = \sqrt{\left(D_h \cdot \frac{\Delta p}{p_s} + x_h \right)^2 + x_v^2},$$

θ_1 is replaced by θ_1^n in above cooling force formulas for practical calculation. When the condition $r > r_b$ is met on a certain passage through the cooling section, the cooling force is set to zero since the ion is outside the electron beam.

The momentum spread $\frac{\Delta p}{p_s}$ of the ion and its coordinates in transverse phase space (x_j, θ_j) are recorded at the exit of cooling section on each turn. The point (x_j, θ_j) is positioned on an ellipse, and the elliptic equation is connected with local Twiss parameters by

$$\gamma_i x_j^2 + 2\alpha_j x_j \theta_j + \beta_j \theta_j^2 = \epsilon_j,$$

where ϵ_j is the Courant-Snyder invariant [6], and $\pi\epsilon_j$ stands for beam emittance.

On the basis of the above principle, a computer program is made to simulate the electron cooling process of a typical ion beam $^{40}\text{Ar}^{18+}$ at the injection (25 MeV/u) into HIRFL-CSR. Parameters involved in the simulations are listed in Table 1.

3. SIMULATION RESULTS AND DISCUSSION

Figure 2 shows the obtained evolution of momentum spread and emittances with time. The horizontal and vertical emittances exhibit nearly the same variations. The momentum spread of the ion is decreased in oscillation, and the oscillation envelope corresponds to the beam momentum spread. Furthermore, the nonlinear feature of the cooling force as a function of ion velocity influences significantly the behavior of ϵ_j and $\frac{\Delta p}{p_s}$ vs. time. When they become small, the cooling rate increases drastically, which leads to a fast reduction of these quantities.

Table 1
The parameters used in the simulation.

Storage ring parameters	
Ring perimeter	141.051 m
Length of cooling section	2.7 m
Betatron tune	$Q_h = 3.4516, Q_v = 2.8893$
β value in cooling section	$\beta_h = 7.311 \text{ m}, \beta_v = 8.981 \text{ m}$
α value in cooling section	$\alpha_h = \alpha_v = 0$
Dispersion in cooling section	$D_h = 0.0 \text{ m}$
Chromaticity	$\xi_h = -4.907, \xi_v = -3.988$
Transition γ_r	4.359
RF voltage amplitude	400 V
RF harmonic number	1
Period of synchrotron oscillation	2.87 ms
Electron beam parameters	
Electron energy	13.71 keV
Average velocity	$6.81 \times 10^7 \text{ m/s}$
Electron beam radius	2.5 cm
Electron beam current	1.2 A
Electron density	$5.60 \times 10^7 / \text{cm}^3$
Transverse temperature	0.2 eV
Longitudinal temperature	$0.19 \times 10^4 \text{ eV}$
Transverse rms velocity	$1.88 \times 10^5 \text{ m/s}$
Longitudinal rms velocity	$3.14 \times 10^3 \text{ m/s}$
Solenoid field strength	1000 Gauss
Ion beam parameters before cooling	
Ion species	$^{40}\text{Ar}^{18+}$
Energy	25 MeV/u
Transverse emittance	$25 \pi \text{ mm} \cdot \text{mrad}$
Momentum spread	$\pm 1.5 \times 10^{-3}$

For the sake of explicitness, hereafter one defines an equilibrium cooling time τ , i.e., the time duration needed to cool the ion beam from the initial emittance to a specified value of $\pi \epsilon_{h,v} = 0.5 \pi \text{ mm} \cdot \text{mrad}$, to distinguish the e^{-1} cooling time defined in the introduction.

3.1. Effects of the electron beam space charge

In order to investigate the electron beam space charge effect, one changes only the neutralization factor f_n , keeping other parameters unvaried, where the dispersion is free in the cooling section. The simulation results are shown in Fig. 3 for $f_n = 0, 50, \text{ and } 90\%$, respectively. It can be seen from the figure that neutralizing the space charge of the electron beam makes cooling faster, especially in the longitudinal case.

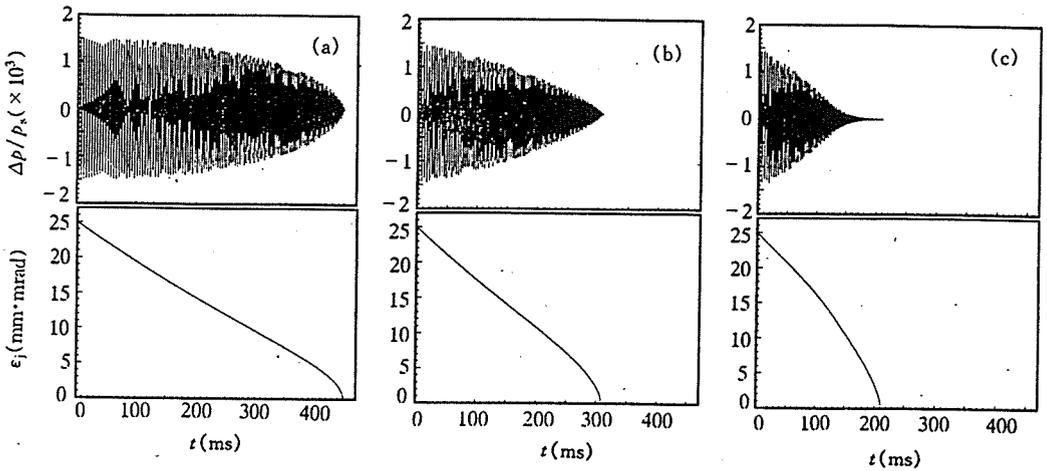


Fig. 2
 Variations of the momentum spread and transverse emittances with time.
 (a) $f_n = 0, f_n = 50\%$, (c) $f_n = 90\%$.

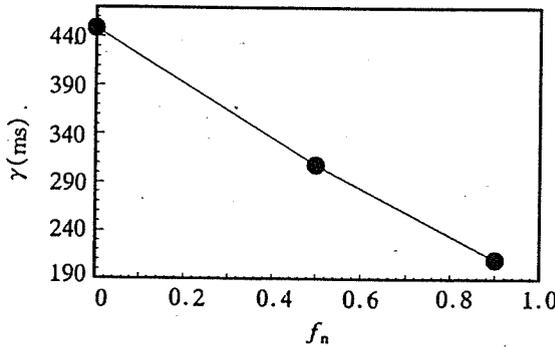


Fig. 3
 The cooling time τ vs. the neutralization factor f_n of electron beam space charge.

As demonstrated in Eq. (10) and Fig. 4, the profile of the electron momentum deviation due to the space charge is a parabola, and the parabola becomes narrower with the lowering of f_n . When the ion traverses the cooling section with momentum deviation less than zero, supposing it is positioned at point *A* of Fig. 4 due to the betatron oscillation and (or) dispersion, the longitudinal velocity difference between the ion and the electron at the same position may be depicted by the line segments AB_1 , AB_2 , and AB_3 , obviously $AB_1 > AB_2 > AB_3$. As a larger velocity difference leads to a smaller cooling force, the parabola gets narrower, i.e., f_n is smaller, the cooling time becomes longer.

3.2. Influence of the dispersion in the cooling section

The dispersion in the cooling section places its influence on the cooling process by joint action with the neutralization factor. So, simulation is performed by varying both the dispersion D_h and neutralization factor f_n with other parameters remaining unchanged (the electron beam current is 1.2 A). The simulation results are illustrated in Fig. 5 together with the relevant f_n and D_h values.

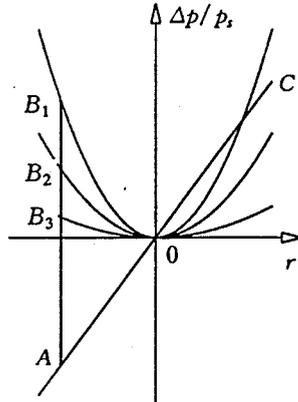


Fig. 4

Parabola profile of the electron momentum due to the space charge effect. The straight line AC represents the ion momentum dispersion in the cooling section.

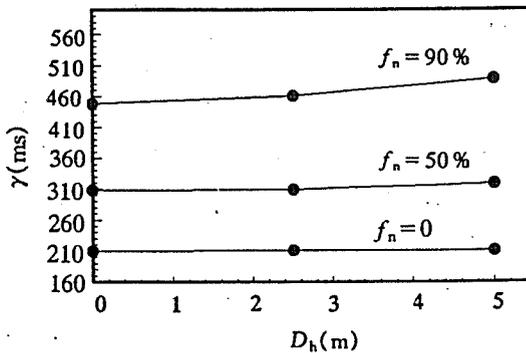


Fig. 5

Combined influences of dispersion D_h and the neutralization factor f_n on the cooling time τ .

Under the conditions that the electron beam current is 1.2 A and the space charge has been neutralized by at least 50%, the cooling speed is barely influenced even if a dispersion of 5.0 m exists in the cooling section. This is mainly due to the existence of synchrotron oscillation which makes the ion go through the cooling section with either positive or negative momentum deviation periodically. In the case of negative value, the cooling speed gets slower as explained above, but its positive deviation helps to fasten the cooling. As a whole, the influence of the dispersion is unessential, and the cooling proceeds faster as long as the electron beam is neutralized. On the other hand, non-zero dispersion causes a horizontal beam spread if the electron acceleration voltage fluctuates (the high voltage ripple), which restricts the reachable lowest temperature of the cooled ion beam [3]. It also leads to an unstable region for the ion beam. All in all, zero dispersion in the cooling section is mandatory in the HIRFL-CSR.

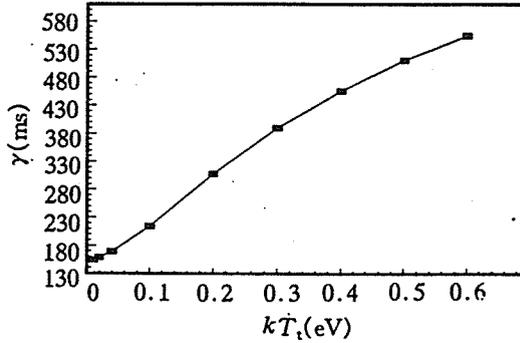


Fig. 6
The cooling time τ as a function of the electron beam transverse temperature kT_t .

3.3. Influence of electron beam transverse temperature

The transverse temperature of the electron beam is one of the critical factors that influence the cooling speed. Assuming the transverse temperatures of 0.01, 0.02, 0.04, 0.1, 0.2, 0.4, 0.5, and 0.6 eV, respectively, with other parameters remaining unchanged ($f_n = 50\%$), the resultant cooling time τ is shown in Fig. 6. It is evident that an electron beam with low transverse temperature is capable of shortening the cooling time.

4. CONCLUSION

We demonstrate the simulation results of the electron cooling process for a heavy ion beam in HIRFL-CSR. Dependence of the cooling time on some factors such as the dispersion of the ring, the transverse temperature, and space charge effect of electron beam are illustrated.

Strictly speaking, a nonlinear force may deform the phase ellipse of an ion beam, and make particles which are on the same elliptic curve initially have a different locus in phase space. However, results from the simulation of 300 particles (200 of them located on an identical ellipse in the beginning) demonstrate that the phase space deformation due to the nonlinear electron cooling force is quite small, and the maximum relative difference of the elliptic areas of these 200 particles is less than 2%. Therefore a single particle is used in the above simulation.

In addition, we also simulate the cooling processes of C^{6+} and S^{16+} beams of 11.1 MeV/u at the TSR, Heidelberg. The obtained results are in agreement with the measurements.

Finally, we may conclude from the simulation results that neutralizing the space charge of the electron beam with a much lower transverse temperature is preferable for faster cooling. Thus, the adiabatic expansion scheme is desired for the design of the electron gun of the HIRFL-CSR e-cooler.

ACKNOWLEDGMENTS

The authors wish to express their gratitude to Prof. I.N. Meshkov from Dubna, Russia, for providing valuable references, and T. Katayama from INS, Tokyo University, for helpful discussions.

REFERENCES

- [1] M. Steck *et al.*, GSI Report, GSI-95-05, (1995), p. 33.
- [2] I.N. Meshkov *et al.*, Heavy Ion Storage Ring Complex K4-K10, A Technical Proposal, Dubna, 1992, p. 85.

- [3] H. Poth, *Phys. Rep.*, **196**(1990), p. 137.
- [4] A.Yu Lavrentev and I.N. Meshkov, private communication, 1995.
- [5] J. Le Duff, CERN 94-01 (1994), p. 289.
- [6] E.D. Courant and H.S. Snyder, *Annals of Physics*, **3**(1958), p. 1.
- [7] I.N. Meshkov, *Phys. Part. Nucl.*, **25**(1994), p. 631.
- [8] Ya.S. Derbenev and I.N. Meskov, CERN 77-08 (1977).
- [9] T.J.P. Ellison, thesis, U. of Indiana, Bloomington, Indiana (1991).